Lithuanian Journal of Physics, Vol. **52,** No. 1, pp. 1–9 (2012)

INTERACTION OF SEMICONDUCTOR SAMPLE WITH TE_{10} MODE IN DOUBLE RIDGED WAVEGUIDE

Ž. Kancleris and P. Ragulis

Semiconductor Physics Institute, Center for Physical Science and Technology, A. Goštauto 11, LT-01108 Vilnius, Lithuania

E-mail: kancleris@pfi.lt

Received 1 January 2012; revised 29 January 2012; accepted 1 March 2012

An interaction of a semiconductor sample inserted in the centre of a double ridge waveguide between its metal ridges with TE_{10} mode was investigated. A three-dimensional finite-difference time-domain method was applied for the calculation of the electromagnetic field components in the waveguide section with a semiconductor sample. The average electric field strength in the sample and the reflection coefficient were determined. This sample is considered a prototype of the sensing element (SE) of a resistive sensor (RS) the performance of which is based on electron heating effect in the semiconductor. The optimal dimensions and specific resistance of the SE have been found, providing frequency response as flat as possible for the RS in the WRD250 waveguide covering the frequency range of 2.60–7.80 GHz.

Key words: electromagnetic wave, double ridged (H-type) waveguide, TE mode, finite-difference time-domain method, semiconductor obstacle, resistive sensor

PACS: 41.20.-q, 07.50.-e, 07.57.Kp

1. Introduction

A resistive sensor (RS) is a device the performance of which is based on electron heating effect in semiconductors. The sensing element (SE) of a RS is placed into a transmission line, usually waveguide. The microwave electric field heats electrons in the SE, its resistance increases and by measuring this resistance change the microwave pulse power in the waveguide is determined. Since the strong electric field should be applied to a semiconductor sample to heat electrons, a RS found its application for high power microwave (HPM) pulse measurement [1]. Comparing a RS with a semiconductor diode, which is also sometimes used for HPM pulse measurement, some advantages of the RS can be mentioned: the RS measures HPM pulses directly, produces a high output signal, is overload resistant and demonstrates perfect long-term stability [1].

Several types of RSs with a flat frequency response in the rectangular waveguide have been designed and realised: the cross-waveguide type RS with the SE the height of which is equal to the narrow wall of the waveguide [2], the RS with a diaphragm where the SE is placed between a thin metal foil and the wide wall of the waveguide [3, 4], and the RS with two sensing elements the height of which is much less than the narrow wall of the waveguide [5, 6]. The main disadvantage of the waveguide type RS is a narrow frequency range where the particular sensor can be used. This range is limited by the pass band of the traditional rectangular waveguide. A double ridged waveguide shown in Fig. 1 is very attractive from this point of view, since its pass band is more than two times wider than the rectangular waveguide. As one can see from the figure, the double ridged waveguide is a traditional rectangular waveguide containing two metal inserts or ridges. The cross-sectional view of a double ridge waveguide is suggestive of letter H, so sometimes it is named an H-type waveguide. The region of the waveguide between metal ridges is usually named a gap region whereas side regions are named the troughs.

In our previous paper [7] we investigated one of the possible realisations of a RS in a double ridged waveguide. As in [5, 6] the layout with two sensing elements was considered. They were placed in the gap region on the surface of the metal ridge. Although electrophysical parameters of SEs providing a sufficiently flat frequency response have been found, the calculated sensitivity of the RS was very low. Having in mind that due to a smaller distance between metal surfaces in the gap region the maximum pulse power transmitted through the double ridged waveguide is lower, the practical realisation of such RS is doubtful. In the present paper we are considering interaction of a semiconductor sample with TE_{10} mode in a double ridge waveguide. The sample is inserted in the centre of the double ridged waveguide and covers the gap region of it. It is analogous to the cross-waveguide type RS in a rectangular waveguide demonstrating high sensitivity and flat frequency response [2]. These facts stimulated our investigations with a purpose to find a more acceptable layout of the SE for the measurement of microwave pulse power propagating in a double ridged waveguide.

2. Double ridged waveguide

A cross-sectional view of a double ridged waveguide and its characteristic dimensions are shown in Fig. 1. One of the earliest papers calculating the cut-off frequency and impedance of ridged waveguides was authored by Cohn [8]. Since then a lot of research was done and the first military standards were approved in 1966. In the present work we performed an investigation with a semiconductor bar inserted into the WRD250 waveguide, the parameters of which are collected in Table 1 [9]. In the table, characteristic dimensions of the waveguide, the lowest and highest passing frequencies, their ratio and the maximum pulse power are presented. As one can see from the table the ratio $f_{max}/f_{min} = 3$, whereas for a traditional waveguide this ratio is 1.5. A double ridged waveguide itself covers more than two bands of a traditional waveguide; therefore, when using a double ridged waveguide the frequency range where the RS operates can be significantly widened. Due to a smaller gap between metal walls the maximum power that can be transmitted through a double ridged waveguide decreases but according to the last column of Table 1 over a hundred kW pulse can be conveyed.

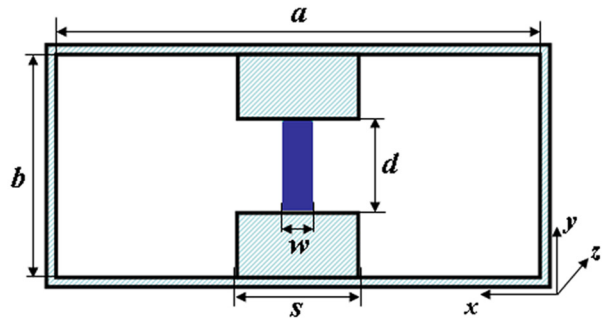

Fig. 1. Sectional view of a double ridged waveguide with the semiconductor sample mounted between metal ridges. Dimension of the sample in z direction is l.

Early calculations of the cut-off frequency of a double ridged waveguide were based on the transverse resonance method [10]. A closed form approximation for the critical wavelength of the dominant mode in a double ridged waveguide was obtained in [11]:

$$\lambda_c = 2a\delta\left[1+\frac{4b}{\pi\delta a}\left(1+0.2\sqrt{\frac{b}{\delta a}}\right)\right.$$
$$\left.\times\ln\csc\frac{\pi d}{2b}+\left(2.45+0.2\frac{s}{a}\right)\frac{bs}{ad\delta}\right]^{\frac{1}{2}}, \qquad (1)$$

where $\delta = 1 - s/a$.

The power flow in the waveguide at finite frequency can be expressed in terms of the power flow at infinite frequency:

Table 1. Double ridged waveguide WRD250.

	a, mm	b, mm	s, mm	d, mm	f_{min}–f_{max}, GHz	f_{max}/f_{min}	P_{max}, kW
WRD250	42.0	18.2	11.2	3.8	2.60–7.80	3.0	120

$$P = P_\infty \sqrt{1-\left(\frac{\lambda}{\lambda_c}\right)^2}, \tag{2}$$

where λ is the wavelength of electromagnetic wave in free space. As it was shown in [12] P_∞ can be expressed as follows:

$$P_\infty = \frac{E_0^2 d\lambda_c}{2\pi Z_0}\left\{\frac{2d}{ak}\cos^2\frac{\pi\gamma}{k}\times \ln\csc\frac{\pi d}{2d}\right.$$

$$+\ \frac{\pi\gamma}{2k}+\frac{1}{4}\sin\frac{2\pi\gamma}{k}+\frac{d}{b}\cdot\frac{\cos^2(\pi\gamma/k)}{\sin^2(\pi\delta/k)}$$

$$\left.\times\ \left[\frac{\pi\delta}{2k}-\frac{1}{4}\sin\frac{2\pi\delta}{k}\right]\right\}, \tag{3}$$

where E_0 is an amplitude of electric field in the centre of the empty waveguide, Z_0 is an impedance of free space, and the rest parameters in Eq. (3) are the following:

$$k = \lambda c/a,\ \gamma = s/a,\ \delta = (1-\gamma). \tag{4}$$

Making use of Eqs. (1)–(4) one can easily calculate the critical wavelength in a double ridge waveguide and knowing E_0 the transmitted power in it.

The closed form of the description of electric and magnetic fields in a double ridged waveguide has been found by Gestinger [13]. It is based on retaining a single mode in a gap region with the components E_y, H_x and H_z, the amplitudes of which depend on coordinate x in a similar way as in a rectangular waveguide. In a trough region the amplitudes E_x, E_y, H_x, H_y and H_z are expanded in infinite series of modes. It should be pointed out that the fields fail at the boundary between the two regions but are adequate everywhere else and provide a reasonable description of power flow [10]. The failure at the boundary has its origin in the use of a single mode in the ridge gap. It is obvious that for TE_{10} mode $E_z = 0$. In our calculations we account for up to 100 terms in series at a trough region.

3. Resistive sensor

The performance of a RS is based on electron heating effect in semiconductors. Therefore, its SE is actually resistor made from n-Si with Ohmic contacts on the ends. In the present paper we consider a SE the length of which is equal to the gap between ridges in a double ridged waveguide. The SE is schematically shown in Fig. 1. Its height h corresponds to d, the width is denoted as w and the length in a wave propagation direction is l. The electric field of the microwave pulse heats electrons in the SE and its resistance increases. Thus, by measuring this resistance change the microwave pulse power in the transmission line is determined.

The general requirements for the n-Si sample that can serve as a SE can be formulated as follows: a SE should not cause considerable reflections in the waveguide, hence the value of the voltage standing wave ratio (VSWR) is set at < 1.5; DC resistance of the RS should not exceed 1 kΩ enabling measurement of microsecond duration microwave pulses; the frequency response of the RS in the waveguide's frequency band should be as flat as possible.

Since under the influence of a strong electric field the resistance of the SE changes, a relative resistance change $\Delta R/R$ of the SE in the microwave electric field characterises the sensitivity of the RS in the best way. Taking into account Eq. (2), the sensitivity of the RS can be expressed in the following way:

$$\zeta = \frac{\Delta R/R}{P} = \frac{\Delta R/R}{P_\infty\sqrt{1-(\lambda/\lambda_c)^2}}. \tag{5}$$

In the frequency range of the WRD250 waveguide the electron heating inertia in n-Si does not manifest itself; therefore, a relative resistance change in the so-called warm electron region [14] can be expressed as

$$\frac{\Delta R}{R} = \frac{3}{2}\beta\langle E\rangle^2, \tag{6}$$

where β is a warm electron coefficient defining deviation of the current–voltage characteristic from Ohm's law, and $\langle E\rangle$ is an average of the electric field amplitude in the SE. By inserting Eq. (6) into Eq. (5) one can get the following expression for the calculation of the sensitivity of the RS in a double ridged waveguide:

$$\zeta = \frac{3\beta E_0^2}{2P_\infty} \cdot \frac{1}{\sqrt{1-(\lambda/\lambda_c)^2}} \cdot \frac{\langle E\rangle^2}{E_0^2}. \qquad (7)$$

In Eq. (7) three multipliers are distinguished. The first one is independent of frequency. The second multiplier in the obtained expression accounts for the fact that due to wave dispersion in the waveguide even at the same power level transmitted through the waveguide, the electric field strength in it decreases with frequency leading to a decrease of sensitivity. The third multiplier is a square of the average of the electric field in the SE normalised to the amplitude of the electric field in the centre of the empty ridged waveguide.

As one can see from expression in Eq. (7), in order to get the sensitivity of the RS independent of frequency, the electrophysical parameters of the SE have to be chosen in such a way that electric field amplitude should increase with frequency, compensating the decrease of sensitivity due to dispersion in the waveguide. A desirable normalised dependence of the average electric field in the "ideal" SE on frequency calculated from Eq. (7) is shown in Fig. 2. It is seen that in the frequency range from 2.6 up to 7.8 GHz electric field should increase by a factor 1.22 and a steeper increase of $\langle E\rangle$ in the frequency range 2.6–5 GHz is desirable.

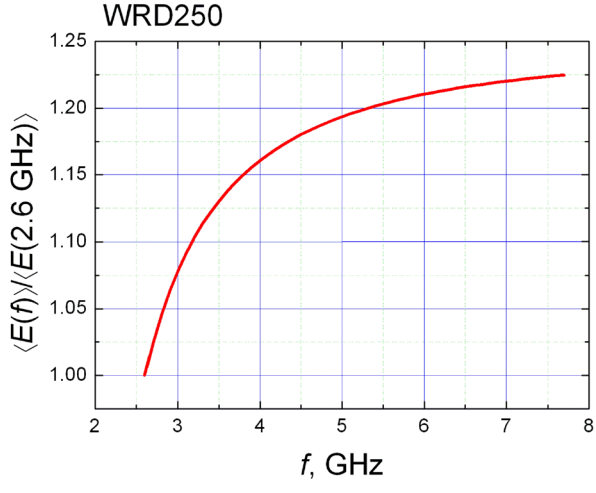

Fig. 2. Dependence of the average electric field in the sample on frequency for the ideal sensor the sensitivity of which should be independent of frequency in the WRD250 waveguide.

4. Calculation method

We used a finite-difference time-domain (FDTD) method for the calculation of the electromagnetic field components in the structure [15]. Using this method all volume of interest is filled with points where components of electric and magnetic field are calculated. Points in the volume are shifted with respect to each other by a half step. Therefore, each component is actually calculated in a different place. Time and coordinate derivatives in Maxwell equations are changed to finite differences and simple formulas are obtained to calculate new values of electromagnetic field components from older ones. In a time domain, calculations are performed each half time step. Using old values of H components the new E components are determined and from them in the next step the newest H components are found out. Such calculation scheme provides h^2 accuracy in both space and time domains. The details of the application of the FDTD technique can be found in [16].

The section of a double ridged waveguide with a SE inside has been modelled. Non-reflecting boundary conditions at both ends of the section are satisfied. At a few grid points from the left side of the structure the regular TE_{10} wave is excited. A continuous-wave excitation was applied in order to simulate the injected wave. The amplitudes of electric and magnetic fields were calculated during each period. The values of E_y calculated in the current period were compared with the ones calculated one period earlier in order to determine whether computation can be terminated. The largest allowed difference was set to be 3% for the termination of calculations. The magnetic field in our calculations was measured in electric field units $H = H' \cdot Z_0$, where H' is the magnetic field measured in A/m. The field amplitudes were normalised to a maximum of the electric field in an empty waveguide E_0. We used dimensionless coordinates and time; therefore, coordinate and time steps are expressed as $\Delta x/a$, $\Delta y/a$, $\Delta z/a$, and $\Delta t \cdot c/a$, where c is the velocity of light in free space. In our calculation we accept that the relative dielectric constant of Si is $\varepsilon = 11.9$. The values of warm electron coefficient β for different specific resistance n-Si samples at room temperature are known. Therefore, by calculating the average electric field in the SE and making use of Eq. (7) the sensitivity of the RS is determined. The above-described procedure has been used for

the calculation of sensitivity of the RS in a rectangular waveguide. A good coincidence between the measured and calculated values obtained in [3, 4, 6] allows us to hope that analogous calculations for the RS in a double ridged waveguide will also give reliable results.

As follows from Table 1, dimensions of the WRD250 waveguide expressed in millimetres have tenths of mm; therefore, for exact modelling of the waveguide window a very small step should be used. For the modelling with a larger step we used a cruder model of the waveguide approximating its dimension to integer numbers, namely: $a = 42$ mm, $b = 18$ mm, $s = 11$ mm, $d = 4$ mm. We assume that the model used allows us to elucidate general peculiarities of electromagnetic field distribution in the section of the double ridged waveguide with a SE using less computer resources. For this reason we are also modelling only the half window of the waveguide with the sample since this structure is symmetric in respect of the plane crossing the centre of the waveguide.

A typical distribution of the components of electric and magnetic fields in the modelled section with a SE in the horizontal plane situated at a distance of 1 mm from the metal ridge is shown in Fig. 3. The dimensions of the SE are $h \times w \times l = 4 \times 1.5 \times 3$ mm^3, specific resistance $\rho = 50$ Ω cm. A continuous wave is injected at $x = 0$, on the other side of the waveguide the non-reflecting boundary conditions are satisfied. It is seen that in the gap region ($x > 0.37$) the components E_y, H_x and H_z propagate. The component H_z is zero in the centre of the waveguide, whereas the components E_x and H_y (the latter is not shown in the figure) do not propagate in the gap region. Considering component E_x one can observe that near the edge of the metal ridge the spike is seen. The same spike is characteristic of the component H_y. It seems that

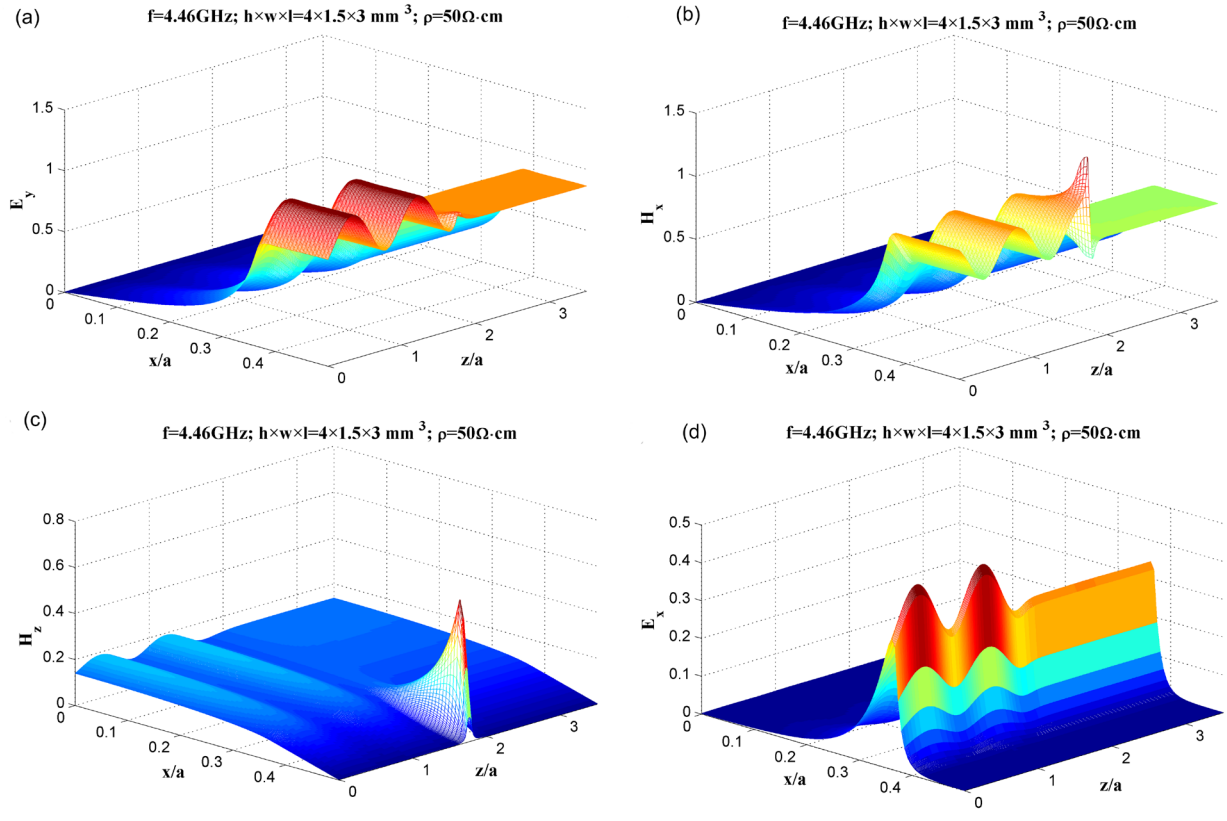

Fig. 3. Calculated dependence of components of electric and magnetic fields in a double ridged waveguide with a sample. Fields are shown in a plane 1 mm apart from the metal ridge. Parameters of the sample: $h \times w \times l = 4 \times 1.5 \times 3$ mm^3, $\rho = 50$ Ω cm, $\varepsilon = 11.9$, $f = 4.46$ GHz; (a) E_y, (b) H_x, (c) H_z, (d) E_x. Field components are normalised to E_0.

those spikes appear due to inconsistence of gap and trough regions. As it was mentioned in Section 2, a single mode propagates in the gap region whereas the multimode regime is characteristic of the trough region [10]. According to [10] this inconsistence should not have influence on wave propagation in a double ridged waveguide.

Since a SE is homogeneous in y direction, E_z component does not appear. As it is seen from Fig. 3(c) H_z component is strongly perturbed by the SE. Before it, a partly standing wave is formed from which the reflection coefficient is determined. For this particular case the VSWR is 1.48. Each component of electromagnetic field in the waveguide section was calculated at 1.9 million points. In this particular case to reach the desirable solution 8 periods of oscillations were modelled. One period on a 3.4 GHz, 8 core, 16 GB memory computer lasts roughly 3 min. Performing analogous calculation at 2.6 GHz is more laborious, since due to increased wavelength the number of points for each component increases up to 4.4 million and calculation of one period lengthens to 15 min.

5. Results and discussion

We started our investigation from a dielectric sample. The dependences of the reflection coefficient and the average electric field in the sample on its length l at different width w at 6.55 GHz are shown in Fig. 4. It is seen that the reflection coefficient is an

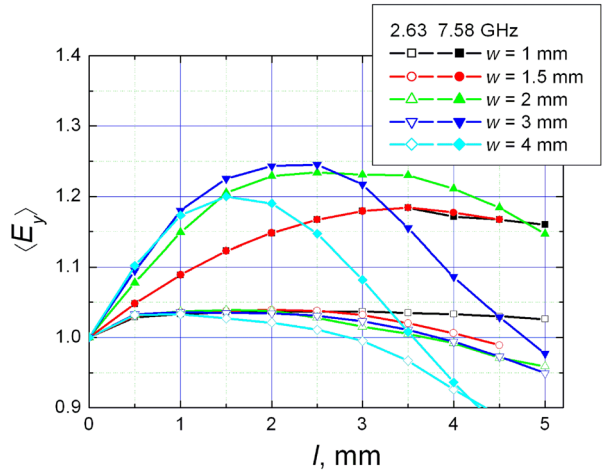

Fig. 5. Dependence of electric field strength in the dielectric sample on its length l for different width w at the frequency of 2.63 and 7.58 GHz.

oscillating function of length that is characteristic of the Fabry–Perot resonance. A strong decrease of the reflection coefficient occurs when the length of the sample is equal to the integer number of $\lambda_d/2$, where λ_d is the wavelength in the sample. One should have in mind that in this case the electromagnetic wave propagates not only through the semiconductor but also through the waveguide. This is the reason why the resonance position depends on the width of the sample. Considering the dependence of the average electric field $\langle E_y \rangle$ in a dielectric sample on its length it is seen that the maximum of the electric field roughly

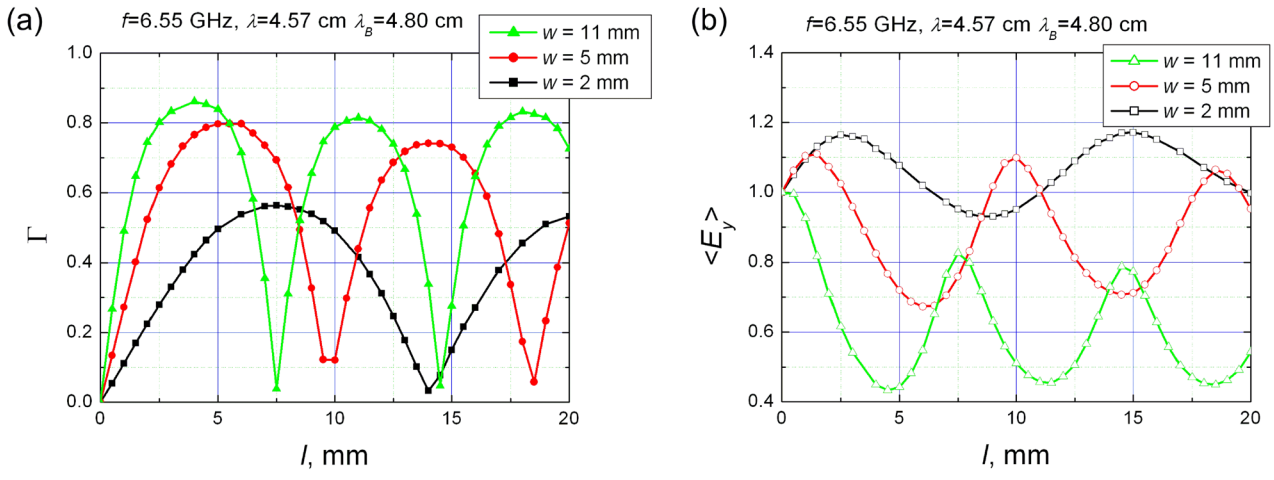

Fig. 4. Calculated dependence of (a) reflection coefficient and (b) average electric field in the dielectric sample on the length of it l at different width w. Parameters of the sample: h = 4 mm, $\rho = \infty$ Ω cm, f = 6.55 GHz.

corresponds to the resonance position whereas the minimum of $\langle E_y \rangle$ matches up to the maximum of the reflection coefficient. It seems that it should be difficult to employ the Fabry–Perot resonance for the RS design since the resonance is too narrow and it seems to be impossible to establish a low reflection from the sample within the frequency range of the WRD250 waveguide.

Attention was drawn to the increase of the electric field in the sample at small l when $w = 2$ mm. It is seen that this effect disappears when w increases. We calculate the dependence of the average electric field in the dielectric sample on its length at the lowest and the highest frequencies of the pass band of WRD250. Calculation results are shown in Fig. 5. It is seen that at $f = 2.63$ GHz, the increase of the average electric field is negligible whereas at the highest frequency a clear growth of the electric field is observed. The maximum value of the electric field at 7.58 GHz is observed when $w = 3$ mm. By choosing the width and length of the dielectric plate $w \times l = 2 \times 3$ mm^2 it is possible to get the increase of the electric field by a factor 1.22 which is characteristic of an ideal sensor. Unfortunately, such a sample demonstrates a very large reflection at a higher frequency (VSRW = 2.4), therefore for the SE the narrower samples should be chosen.

From the variety of dimensions and specific resistances of the investigated samples we have chosen 1 mm width samples of low ($\rho = 10$ Ω cm) and high ($\rho = 50$ Ω cm) specific resistance, which are the most suitable for SE manufacturing. The calculated normalised average electric field in the SE dependences on frequency for $\rho = 10$ Ω cm and different length samples are shown in Fig. 6. As one can see from the figure, for a short sample the increase of the electric field with frequency is too small to get a flat frequency response, but by increasing l the average electric field dependence on frequency approaches the ideal. It confirms the results of sensitivity dependence on frequency shown in Fig. 7 (a). They were calculated with the help of Eq. (7) by using the known values of the average electric field in the SE and using $\beta = 6.1 \cdot 10^{-8}$ cm^2/V^2.

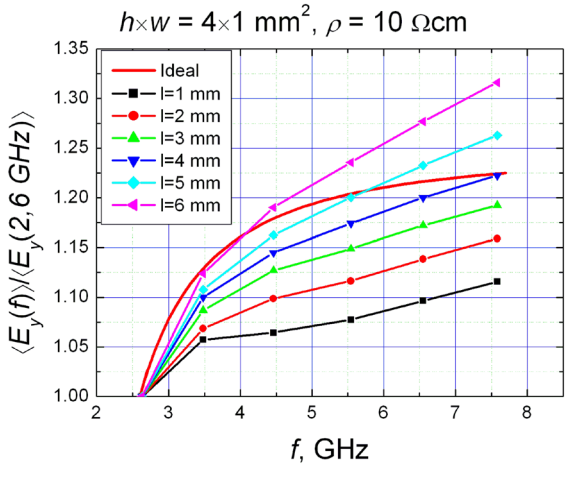

Fig. 6. Dependence of normalised electric field strength in the sample on frequency for different sample length l: $h \times w = 4 \times 1$ mm^2, $\rho = 10$ Ω cm, $\varepsilon = 11.9$. Symbols show calculation results, solid line corresponds to the ideal sensor, the sensitivity of which is independent of frequency.

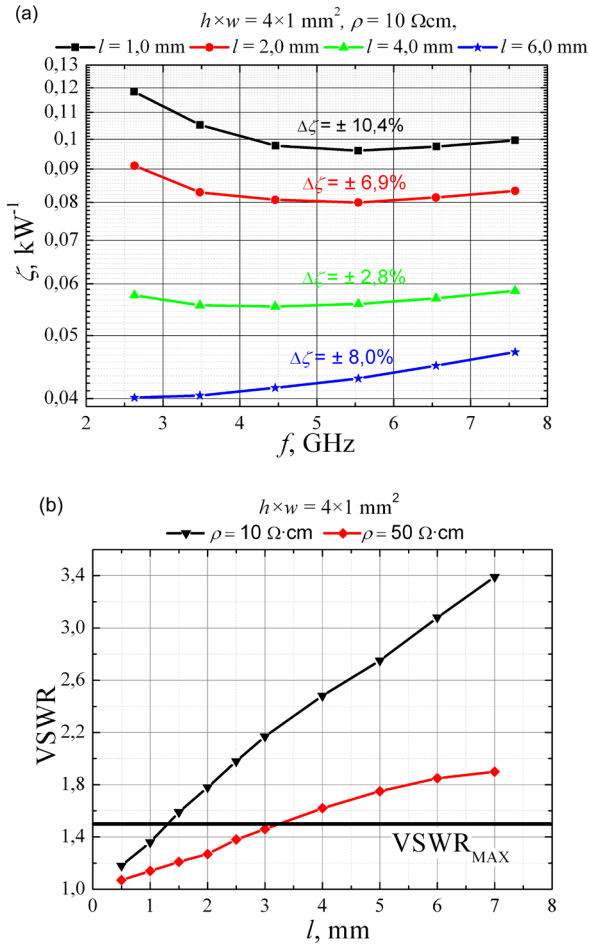

Fig. 7. (a) Calculated dependence of sensitivity on frequency for different length samples made from $\rho = 10$ Ω cm. (b) Dependence of the maximum value of VSWR on length l when $\rho = 10$ and 50 Ω cm. Dimensions of the sensor $h \times w = 4 \times 1$ mm^2, $\varepsilon = 11.9$.

It is seen that by increasing l the absolute value of sensitivity decreases. The smallest calculated sensitivity variation (±2.8%) of the SE was found at l = 4 mm. Having in mind a wide frequency range of the WRD250 waveguide it should be an excellent result. Unfortunately, as follows from Fig. 7 (b), such a sensor is of little use due to a very large reflection. Its VSWR is roughly 2.5 and it is not acceptable for a measuring device. From the investigated samples, a sensor with cross-sectional dimensions $w \times l = 1 \times 1$ mm^2 can be considered a prototype of the SE. Its sensitivity variation is ± 10.4%, VSRW < 1.4, and DC resistance is 400 Ω.

We also investigated a ρ = 50 Ω·cm specific resistance SE. The calculation results are shown in Fig. 8. In the calculations the value $\beta = 6.4 \cdot 10^{-8}$ cm^2/V^2 was used. Taking into consideration the variation of sensitivity, reflection coefficient and DC resistance, it was found that the SE with cross- sectional dimensions $w \times l = 1 \times 3$ mm^2 is preferable. The calculated sensitivity variation is roughly ±12%, VSRW < 1.5, and DC resistance is 670 Ω. As one can see from the figure, the SE the length of which is l = 5 mm demonstrates even a smaller sensitivity variation, namely ±8.1%. As in the case of a lower specific resistance SE, its reflection is too large (ref. to Fig. 7 (b)) and it cannot be used as a prototype for the RS. By comparing sensitivities of the samples chosen as prototypes of the SE shown in Fig. 7 (a) and Fig. 8 we can see that the sensitivity of a larger specific resistance SE is roughly 20% higher. By comparing the values of the sensitivity of the RS calculated here with those found earlier [7] it should be noted that the cross-waveguide layout provides sensitivity about three orders of magnitude larger than the layout with two sensing elements does. The main reason of a strong decrease of sensitivity of the RS [7] is the decrease of the electric field in the SE due to large dielectric constant of Si and fairly low specific resistance (5 Ω cm) used to damp the resonance that occurs in the SE within the considered frequency range.

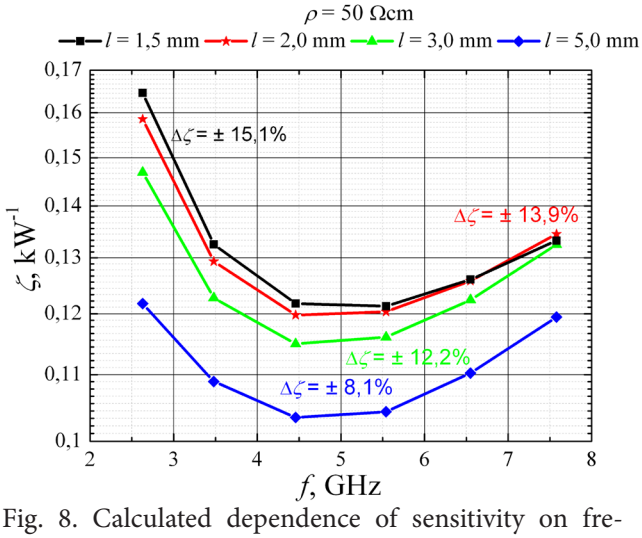

Fig. 8. Calculated dependence of sensitivity on frequency for different length samples: $h \times w = 4 \times 1$ mm^2, ρ = 50 Ω cm, ε = 11.9. Length of the samples is shown in the figure.

6. Conclusions

A cross-waveguide type SE inserted in a double ridged waveguide has been considered in calculating its sensitivity. Although the frequency range of a double ridged waveguide is more than two times wider than that of a traditional rectangular waveguide, at least two configurations of the SE have been chosen for practical realisation. They are: a 10 Ω cm specific resistance SE with cross-sectional dimensions $w \times l = 1 \times 1$ mm^2 and DC resistance 400 Ω, and a 50 Ω cm specific resistance SE with $w \times l = 1 \times 3$ mm^2 and DC resistance 667 Ω. They demonstrate sensitivity variation in the frequency range from 2.6 to 7.8 GHz in the extent of ±10–12%. The sensitivity of the layout of the SE considered in the present paper is roughly 3 orders of magnitude larger than it was found for the layout with two sensing elements earlier [7].

Acknowledgements

This research was funded by a grant MIP-092/2011 from the Research Council of Lithuania.

References

[1] M. Dagys, Ž. Kancleris, R. Simniškis, E. Schamiloglu, and F.J. Agee, Resistive sensor: Device for high-power microwave pulse measurement, IEEE Trans. Antennas Propag. M **43**, 64–79 (2001).

[2] R. Baltušis, M. Dagys, and R. Simniškis, Resistive sensors for high pulse power microwave measurements, in: *Proc. 22nd Euro.Microwave Conf.*, Vol. 1 (Helsinki University of Technology, Helsinki, 1992) pp. 169–173.

[3] Ž. Kancleris, V. Tamošiūnas, M. Dagys, R. Simniškis, and F.J. Agee, Numerical

investigation of resonances within the X-band waveguide type resistive sensors, IEEE Microwave Wireless Components Lett., **16**, 422–424 (2006).
[4] Ž. Kancleris, R. Simniškis, M. Dagys, and V. Tamošiūnas, X-band resistive sensor for high power microwave pulse measurement with flat frequency response, Electron. Letters **44**, 1143–1144 (2008).
[5] Ž. Kancleris, V. Tamošiūnas, M. Dagys, R. Simniškis, and F.J. Agee, Interaction of a semiconductor sample partly filling a waveguide's window with millimetre wave radiation, IEE Proc. Microw. Antennas Propag. **152**, 240–244 (2005).
[6] Ž. Kancleris, R. Simniškis, M. Dagys, and V. Tamošiūnas, High power millimetre wave pulse sensor for W-band, IET Microw. Antennas Propag. **1**, 757–762 (2007).
[7] P. Ragulis, V. Tamošiūnas, Ž. Kancleris, R. Simniškis, and M. Tamošiūnienė, Optimisation of resistive sensor for ridge waveguide, in: *Proc. MIKON-2010*, Vol. 2, ed. B. Levitas (Geozondas, Vilnius, 2010) pp. 714–717.
[8] S.B. Cohn, Properties of ridge waveguide, Proc. IRE **35**, 783–7S8 (1947).
[9] Catalogue of Space Machine & Engineering Corporation: http://www.space-machine.com.
[10] J. Helszajn, Ridge waveguides and passive microwave components, in: *IEE Electromagnetic Wave Series*, Vol. 49, eds. P.G.B. Claricoats and E.V. Jull (The Institution of Electrical Engineering, London, 2000).
[11] W.J.R. Hoefer and M.N. Burton, Close-form expressions for parameters of finned and ridged waveguides, IEEE Trans. Microw. Theor. Tech. **30**, 2190–2194 (1982).
[12] S. Hopfer, The design of ridged waveguides, IRE Trans. Microwave Theory Tech. **3**, 20–29 (1955).
[13] W.J. Getsinger, Ridge waveguide field description and application to directional couplers, IRE Trans. Microwave Theory Tech. **10**, 41–50 (1962).
[14] V. Dienys, Ž. Kancleris, and Z. Martūnas, *Warm Electrons*, ed. J. Požela (Mokslas, Vilnius, 1983) [in Russian].
[15] K.S. Yee, Numerical solution of initial boundary value problems involving Maxwell's equations in isotropic media, IEEE Trans. Antennas Propag. **14**(3), 302–307 (1966).
[16] A. Taflove and S.C. Hagness, *Computational Electrodynamics: The Finite-Difference Time-Domain Method*, 2nd ed. (Artech House, Norwood, 2000).

PUSLAIDININKINIO BANDINIO SĄVEIKA SU TE_{10} MODA H PAVIDALO BANGOLAIDYJE

Ž. Kancleris, P. Ragulis

Fizinių ir technologijos mokslų centro Puslaidininkių fizikos institutas, Vilnius, Lietuva

Santrauka

Darbe tyrinėta puslaidininkinio bandinio sąveika su TE_{10} moda sklindančiu H pavidalo bangolaidžiu. Šio tyrimo pagrindu tikimasi sukurti rezistorinį jutiklį, kurio veikimo principas remiasi elektronų kaitimo efektu puslaidininkiuose ir kuris yra skirtas didelės galios mikrobangų impulsams matuoti. H pavidalo bangolaidis skiriasi nuo įprastinio stačiakampio tuo, kad plačiųjų bangolaidžio sienelių viduryje sumontuojami metaliniai strypai. Tokia bangolaidžio forma gerokai praplečia jo pralaidumo juostą. Aukščiausio ir žemiausio pralaidos dažnių santykis šiame darbe nagrinėto bangolaidžio WRD250 yra 3, kai įprastinio stačiakampio bangolaidžio šis santykis siekia tik 1,5. Taigi panaudojus H pavidalo bangolaidį rezistorinio jutiklio jautriajam elementui įtverti, galima būtų gerokai praplėsti jutiklio dažnių ruožą, kuriame atliekami didelės galios mikrobangų impulsų matavimai.

Strypelio pavidalo bandinys iš n-Si, kuris paprastai naudojamas rezistorinio jutiklio jautriojo elemento gamybai, buvo talpinamas į H pavidalo bangolaidžio centrą tarp metalo strypų, praplečiančių bangolaidžio dažnių ruožą. Maksvelo lygtims spręsti bangolaidžio atkarpoje su patalpintu joje jautriuoju elementu naudojome baigtinių skirtumų laiko skalės metodą. Šio metodo esmė, kad elektromagnetinio lauko sandai yra skaičiuojami taškuose, užpildančiuose visą bangolaidžio sekciją su tiriamuoju bandiniu. Laiko ir erdvės išvestinės Maksvelo lygtyse yra keičiamos į baigtinius skirtumus, gaunamos gana paprastos išraiškos naujesniems elektromagnetinio lauko sandams apskaičiuoti iš senesniųjų.

Pasinaudojus baigtinių skirtumų laiko skalėje metodu, spręstas jutiklio jautraus elemento optimizacijos uždavinys: parinkti tokie jutiklio elektrofizikiniai parametrai (jutiklio matmenys, savitasis laidumas), kad jutiklio jautrio dažninė charakteristika turėtų mažiausią netolygumą, stovinčios bangos koeficientas nuo jutiklio neviršytų 1,5 ir jutiklio varža neviršytų 1 kΩ.

Atlikus tokius tyrimus su jutikliais, įtvertais skersai bangolaidžio lango, tolesnei praktinei realizacijai pasirinkti du jutikliai: 50 Ω cm savitosios varžos jutiklis, kurio matmenys $h \times w \times l = 4 \times 1 \times 3$ mm^3, o varža 667 Ω ir 10 Ω cm savitosios varžos jutiklis, kurio matmenys $h \times w \times l = 4 \times 1 \times 1$ mm^3, o varža 400 Ω. WRD250 bangolaidžio dažnių pralaidumo ruože 2,6–7,8 GHz šių jutiklių apskaičiuotas dažninės charakteristikos netolygumas buvo ±10–12 %.